3). Thus, deletion of JNK2 in macrophages was sufficient to decrease atherogenesis.

Two receptors appear to be essential in foam cell formation and receptor-mediated binding and uptake of modified lipoproteins: CD36 and scavenger receptor A (SR-A) (*20*). Immunofluorescence analyses revealed that expression of CD36 was unchanged in acLDL-stimulated peritoneal $ApoE^{-/-}$ $JNK2^{-/-}$ macrophages (Fig. 4A and fig. S7A). However, analyses with antibodies to SR-A showed increased abundance of this receptor (Fig. 4B and fig. S7B) ($P < 0.01$). Protein immunoblotting confirmed increased abundance of SR-A in protein extracts prepared from macrophages stimulated with acLDL. Amounts of SR-A were not altered in response to acLDL in double knockout or control animals (fig. S7C). $ApoE^{-/-}$ $JNK2^{-/-}$ macrophages formed filopodia-like projections, which were not observed in controls (Fig. 4C). This cellular phenotype is associated with increased adhesion and has been described in macrophages overexpressing SR-A (*21*). To examine whether increased abundance of SR-A in cultured macrophages also occurred in vivo, we used immunohistochemistry to detect SR-A on plaques from $ApoE^{-/-}$ $JNK2^{-/-}$ mice and $ApoE^{-/-}$ control mice. Increased amounts of SR-A were detected in macrophages in plaques of $ApoE^{-/-}$ $JNK2^{-/-}$ mice compared to those of control mice (Fig. 4D).

Alternative splicing results in three types of SR-A transcripts in humans. Occurrence of the Type III SR-A blocks modified LDL uptake (*22*). Therefore, we analyzed the expression of all three splicing variants in macrophages by semiquantitative RT-PCR using specific primers. We could not detect Type III mRNA in macrophages of either genotype. Type I and Type II mRNA was not increased in the absence of JNK2 (fig. S7D). Expression of CD36 or peroxisome proliferator–actived receptor (PPARγ) (*23*), was also not affected. Activation of the well-known JNK target c-jun in aortas from $ApoE^{-/-}$ and $ApoE^{-/-}$ $JNK2^{-/-}$ mice fed either a normal or high-cholesterol diet was not affected, suggesting that c-jun-dependent gene expression was not impaired (fig. S7E). Phosphorylation of SR-A on specific serines is essential for SR-A–dependent processing of modified LDL and for surface expression of SR-A (*24*–*26*). We immunoprecipitated SR-A from total protein extracts of $JNK2^{-/-}$ macrophages and corresponding wild-type cells. Western blotting of immunoprecipitated SR-A revealed an increased amount of SR-A in $JNK2^{-/-}$ cells compared to wild-type cells (Fig. 4, E and F). Blotting with phosphoserine-specific antibody indicated that the amount of serine-phosphorylated SR-A was lower in $JNK2^{-/-}$ extracts even though more SR-A protein was present (Fig. 4E). We confirmed decreased phosphorylation of SR-A after labeling of $JNK2^{-/-}$ macrophages with [^{32}P] orthophosphoric acid (Fig. 4F).

In this study, we provide in vivo evidence that JNK2 is required in a mouse model of atherogenesis. At the molecular level, we propose that JNK2-dependent decrease of SR-A phosphorylation and increase in SR-A abundance may lead to decreased internalization and degradation of receptor-bound modified LDL and as a consequence to reduced foam cell formation. Indeed, macrophage-specific overexpression of SR-A has been shown to be sufficient to reduce atherosclerosis in ApoE-deficient mice (*27*). In conclusion, specific inhibition of JNK2 activity may provide a therapeutic approach to decrease atheroma formation in patients.

References and Notes

1. P. Libby, *Nature* **420**, 868 (2002).
2. C. K. Glass, J. L. Witztum, *Cell* **104**, 503 (2001).
3. S. Gupta *et al.*, *EMBO J.* **15**, 2760 (1996).
4. C. Dong *et al.*, *Nature* **405**, 91 (2000).
5. J. Hirosumi *et al.*, *Nature* **420**, 333 (2002).
6. Z. Han, L. Chang, Y. Yamanishi, M. Karin, G. S. Firestein, *Arthritis Rheum.* **46**, 818 (2002).
7. A. M. Manning, R. J. Davis, *Nature Rev. Drug Discov.* **2**, 554 (2003).
8. A. S. Plump *et al.*, *Cell* **71**, 343 (1992).
9. Y. S. Heo *et al.*, *EMBO J.* **23**, 2185 (2004).
10. M. I. Cybulsky *et al.*, *J. Clin. Invest.* **107**, 1255 (2001).
11. Z. M. Dong, A. A. Brown, D. D. Wagner, *Circulation* **101**, 2290 (2000).
12. G. K. Hansson, P. Libby, U. Schonbeck, Z. Q. Yan, *Circ. Res.* **91**, 281 (2002).
13. D. D. Yang *et al.*, *Immunity* **9**, 575 (1998).
14. H. M. Dansky, S. A. Charlton, M. M. Harper, J. D. Smith, *Proc. Natl. Acad. Sci. U.S.A.* **94**, 4642 (1997).
15. A. Daugherty *et al.*, *J. Clin. Invest.* **100**, 1575 (1997).
16. C. Dong *et al.*, *Science* **282**, 2092 (1998).
17. V. J. Dzau, R. C. Braun-Dullaeus, D. G. Sedding, *Nature Med.* **8**, 1249 (2002).
18. Y. Zhan *et al.*, *Arterioscler. Thromb. Vasc. Biol.* **23**, 795 (2003).
19. A. C. Li, C. K. Glass, *Nature Med.* **8**, 1235 (2002).
20. V. V. Kunjathoor *et al.*, *J. Biol. Chem.* **277**, 49982 (2002).
21. S. R. Post *et al.*, *J. Lipid Res.* **43**, 1829 (2002).
22. P. J. Gough, D. R. Greaves, S. Gordon, *J. Lipid Res.* **39**, 531 (1998).
23. P. Tontonoz, L. Nagy, J. G. Alvarez, V. A. Thomazy, R. M. Evans, *Cell* **93**, 241 (1998).
24. H. Heider, E. S. Wintergerst, *FEBS Lett.* **505**, 185 (2001).
25. L. G. Fong, D. Le, *J. Biol. Chem.* **274**, 36808 (1999).
26. N. Kosswig, S. Rice, A. Daugherty, S. R. Post, *J. Biol. Chem.* **278**, 34219 (2003).
27. S. C. Whitman, D. L. Rateri, S. J. Szilvassy, J. A. Cornicelli, A. Daugherty, *J. Lipid Res.* **43**, 1201 (2002).
28. Macrophages were pulse-labeled with [^{32}P]orthophosphoric acid in sodium-phosphate-deficient culture medium 12 hours before harvesting.

29. We thank P. Lerch who provided us with oxLDL; D. Zhang and P. Meier, who helped us with isolation of aortas; H. Joch and A. Jaschko, who helped us with smooth muscle cell isolation; P. Bargsten, who helped us with bone marrow transplantation experiments; W. Krek and P. J. Gough, with whom we had very fruitful scientific discussions; and R. Eferl, for critical reading. Supported by the Swiss National Science Foundation (grant no. 3100-068118), the European Union (grant no. G5RD-CT-2001-00532), the Bundesamt für Bildung und Wissenschaft, and the Swiss Heart Foundation, and the "Forschungskredit 2003" of the University of Zurich.

Supporting Online Material

www.sciencemag.org/cgi/content/full/306/5701/1558/DC1
Materials and Methods
Figs. S1 to S7
References and Notes

23 June 2004; accepted 13 October 2004

Rise and Fall of the Beringian Steppe Bison

Beth Shapiro,[1,2] Alexei J. Drummond,[2] Andrew Rambaut,[2] Michael C. Wilson,[3] Paul E. Matheus,[4] Andrei V. Sher,[5] Oliver G. Pybus,[2] M. Thomas P. Gilbert,[1,2] Ian Barnes,[6] Jonas Binladen,[7] Eske Willerslev,[1,7] Anders J. Hansen,[7] Gennady F. Baryshnikov,[8] James A. Burns,[9] Sergei Davydov,[10] Jonathan C. Driver,[11] Duane G. Froese,[12] C. Richard Harington,[13] Grant Keddie,[14] Pavel Kosintsev,[15] Michael L. Kunz,[16] Larry D. Martin,[17] Robert O. Stephenson,[18] John Storer,[19] Richard Tedford,[20] Sergei Zimov,[10] Alan Cooper[1,2]*

The widespread extinctions of large mammals at the end of the Pleistocene epoch have often been attributed to the depredations of humans; here we present genetic evidence that questions this assumption. We used ancient DNA and Bayesian techniques to reconstruct a detailed genetic history of bison throughout the late Pleistocene and Holocene epochs. Our analyses depict a large diverse population living throughout Beringia until around 37,000 years before the present, when the population's genetic diversity began to decline dramatically. The timing of this decline correlates with environmental changes associated with the onset of the last glacial cycle, whereas archaeological evidence does not support the presence of large populations of humans in Eastern Beringia until more than 15,000 years later.

Climatic and environmental changes during the Pleistocene epoch [from 2 million years ago (Ma) to 10,000 years before the present (ky B.P.)] played an important role in the distribution and diversity of modern plants and animals (*1*, *2*). In Beringia, local climate

and geology created an ice-free refugium stretching from eastern Siberia to Canada's Northwest Territories (*3*). Periodic exposure of the Bering Land Bridge facilitated the exchange of a diverse megafauna (such as bison, mammoth, and musk ox) supported by tundra-steppe grasses and shrubs (*3*, *4*). Humans are believed to have colonized North America via this route, and the first well-accepted evidence of human settlement in Alaska dates to around 12 ky B.P. (*5*). The latest Pleistocene saw the extinction of most Beringian megafauna including mammoths, short-faced bears, and North American lions. The reasons for these extinctions remain unclear but are attributed most often to human impact (*6*, *7*) and climate change associated with the last glacial cycle (*8*).

Pleistocene bison fossils are abundant across Beringia and they provide an ideal marker of environmental change. Bison are believed to have first entered eastern Beringia from Asia during the middle Pleistocene [marine oxygen isotope stages (MISs) 8 to 6, circa (ca.) 300 to 130 ky B.P.] and then moved southward into central North America during the MIS 5 interglacial period (130 to 75 ky B.P.), where they were distributed across the continental United States (*9*). During this time, Beringian and central North American bison populations may have been periodically separated by glacial ice that formed over most of Canada (*10*, *11*). The timing and extent of genetic exchange between these areas remain unclear (*2*).

The abundance and diversity of bison fossils have prompted considerable paleontological and archaeological research into their use as stratigraphic markers. Extensive morphological diversity, however, has complicated discrimination between even the most accepted forms of fossil bison, and the lack of stratigraphy in Beringian sites has prevented the development of a chronological context. These complications create a complex literature of conflicting hypotheses about bison taxonomy and evolution (*9*, *12*). After a severe population bottleneck, which ocurred only 200 years ago (*13*), two subspecies survive in North America: *Bison bison bison*, the plains bison, and *B. b. athabascae*, the wood bison (*9*, *13*).

To investigate the evolution and demographic history of Pleistocene bison, we collected 442 bison fossils from Alaska, Canada, Siberia, China, and the lower 48 United States (*14*). We used ancient DNA techniques to sequence a 685–base pair (bp) fragment of the mitochondrial control region (*14*). Accelerator mass spectrometry radiocarbon dates were obtained for 220 samples, which spanned a period of >60 ky (*14*).

The association of radiocarbon dates with DNA sequences enables the calibration of evolutionary rates within individual species (*15*). Bayesian phylogenetic analyses produced an evolutionary rate estimate for the bison mitochondrial control region of 32% per million years (My) [95% highest posterior density (HPD): 23 to 41% per My] (*14*). This estimate is independent of paleontological calibrations but agrees with fossil-calibrated rates for cattle of 30.1% per My (*16*) and 38% per My (*17*). This rate was used to calculate the ages of key nodes in the bison genealogy (*14*). The most recent common ancestor (MRCA) of all bison included in this analysis lived around 136 ky B.P. (95% HPD: 164 to 111 ky B.P.). In the majority (66%) of estimated trees, Eurasian bison cluster into a single clade, with a MRCA between 141 and 89 ky B.P. Although

[1]Henry Wellcome Ancient Biomolecules Centre, [2]Department of Zoology, Oxford University, South Parks Road, Oxford OX13PS, UK. [3]Department of Geology and Department of Anthropology, Douglas College, Post Office Box 2503, New Westminster, British Columbia V3L 5B2, Canada. [4]Alaska Quaternary Center and Institute of Arctic Biology, University of Alaska Fairbanks, 900 Yukon Drive, Fairbanks, AK 99775–5940, USA. [5]Severtsov Institute of Ecology and Evolution, Russian Academy of Sciences, 33 Leninsky Prospect, 119071 Moscow, Russia. [6]The Centre for Genetic Anthropology, Department of Biology, Darwin Building, University College London, Gower Street, London WC1E 6BT, UK. [7]Department of Evolutionary Biology, Zoological Institute, University of Copenhagen, Universitetsparken 15–2100 Copenhagen, Denmark. [8]Zoological Institute, Russian Academy of Sciences, 199034 St. Petersburg, Russia. [9]Quaternary Paleontology, Provincial Museum of Alberta, Edmonton, Alberta T5N 0M6, Canada. [10]North-East Scientific Station of Russian Academy of Science, Post Office Box 18, Cherskii, Republic Sakha-Yakutia, Russia. [11]Department of Archaeology, Simon Fraser University, Burnaby, British Columbia V5A 1S6, Canada. [12]Department of Earth and Atmospheric Sciences, University of Alberta, Edmonton, Alberta T6G 2E3, Canada. [13]Canadian Museum of Nature (Paleobiology), Ottawa, Ontario K1P 6P4, Canada. [14]Department of Archaeology, Royal British Columbia Museum, 675 Belleville Street, Victoria, British Columbia V8V 1X4, Canada. [15]Institute of Plant and Animal Ecology, Russian Academy of Sciences, 202 8 Martas Street, Ekaterinburg 620144, Russia. [16]Bureau of Land Management, 1150 University Avenue, Fairbanks, AK 99708 USA. [17]Department of Ecology and Evolutionary Biology, University of Kansas, Lawrence, KS 66045, USA. [18]Alaska Department of Fish and Game, 1300 College Road, Fairbanks, AK 99701, USA. [19]Yukon Paleontologist, Heritage Resources, Yukon Department of Tourism and Culture, Box 2703, Whitehorse, Yukon Territory YTY1A 2C6, Canada. [20]Department of Paleontology, American Museum of Natural History, Central Park West at 79th Street, New York, NY 10024, USA.

*To whom correspondence should be addressed. E-mail: alan.cooper@zoo.ox.ac.uk

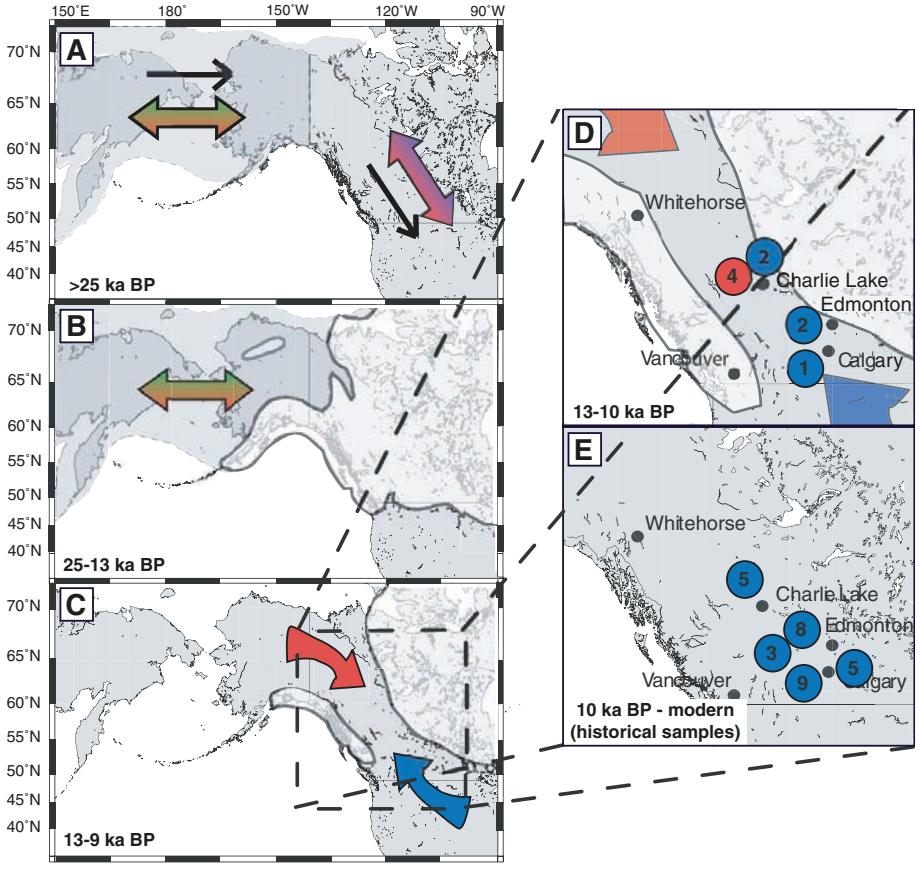

Fig. 1. Distribution of bison in Beringia and central North America through time. (**A** to **C**) Double-headed arrows show gene flow between regions. Black arrows indicate colonization events. Circles in maps (**D**) and (**E**) designate either northern (red) or southern (blue) ancestry and the number of samples from that location.

these two estimates overlap, the age of the MRCA of Eurasian bison was the same as that of the root in 4.8% of 135,000 posterior genealogies (with a Bayes factor of 20.83 that the Eurasian MRCA is not also the MRCA of all clades), suggesting that the Eurasian clade is not the oldest in the tree. This suggests that late Pleistocene bison from the Ural Mountains to northern China are descendants of one or more dispersals from North America. Several North American lineages fall within the Eurasian clade, indicating subsequent asymmetric genetic exchange, predominantly from Asia to North America.

Figure 1A depicts inferred gene flow between bison populations in Beringia and central North America during MIS 3 (~60 to 25 ky B.P.), which is the interstadial period before the Last Glacial Maximum (LGM, ca. 22 to 18 ky B.P.). Bison were continuously distributed from eastern Beringia southward into central North America during this period, before the formation of the Laurentide (eastern) and Cordilleran (western) ice sheets created a barrier to north-south faunal exchange. Although any coalescence between these ice masses was brief (*11*), the absence of faunal remains aged 22 to12 ky B.P. (Fig. 1B) (*18*) indicates that the area was uninhabitable by large mammals during this time. Bison fossils in central North America during the LGM are sparsely distributed across the continent (*9*). DNA could be retrieved only from two specimens from this period, both from Natural Trap Cave, Wyoming (20,020 ± 150 and 20,380 ± 90 ky B.P.). These specimens are not closely related (*14*), indicating that populations south of the ice retained some genetic diversity until the LGM.

The ice sheets began to retreat around 14 ky B.P., forming an ice-free corridor (IFC) through which dispersal between Beringia and North America could occur. The first observed bison haplotypes in the IFC are southern in origin (Fig. 1, C and D), with the oldest specimen being in southern Alberta by 11.3 ky B.P., and others near Athabasca, northern Alberta, by 10.4 ky B.P. This finding is consistent with evidence that the first faunal assemblages and archaeological presence in the IFC were southern in origin (*18–20*). The opening of the northern end of the IFC saw a limited southward dispersal of Beringian bison, with a subset of the northern diversity found near the Peace River (northwestern British Columbia) by 11.2 to 10.2 ky B.P. (Fig. 1C) (*14*). Southern bison are also found in this area around 10.5 ky B.P., making it the only location where post-LGM northern and southern clades occurred at the same time. Subsequent genetic exchange between Beringia and central North America was limited by the rapid establishment of spruce forest across Alberta around 10 ky B.P. (*21*) and by the widespread development of peatland across western and northwestern Canada (*22*). North of these ecological barriers, grasslands were reduced by invading trees and shrubs, yet despite the decrease in quality and quantity of habitat (*3*), bison persisted in eastern Beringia until a few hundred years ago (*14*, *23*).

It has been hypothesized that modern bison descended from Beringian bison that moved south through the IFC after the LGM (*9*, *19*) and have since undergone a decline in diversity due to over-hunting and habitat loss (*13*). In contrast, our data show that modern bison are descended from populations that were south of the ice before the LGM and that diversity has been restricted to at least 12 ky B.P., around the time of the megafaunal extinctions. All modern bison belong to a clade distinct from Beringian bison. This clade has a MRCA between 22 and 15 ky B.P., which is coincident with the separation of northern and southern populations by the western Canadian ice barrier. This clade diverged from Beringian bison by 83 to 64 ky B.P. and was presumably part of an early dispersal from Beringia, as indicated by the long branch separating it from Beringian bison (*14*). If other remnants of these early dispersals survived the LGM, they contributed no mitochondrial haplotypes to modern populations.

Coalescent theory is used to evaluate the likelihood of a demographic history, given plausible genealogies (*24*). Under a coalescent model, the timing of divergence dates provides information about effective population sizes through time. To visualize this for bison, a technique called the skyline plot was used (*14*, *25*). The results showed two distinct demographic trends since the MRCA, suggesting that a simple demographic model, such as constant population size or exponential growth, was insufficient to explain the evolutionary history of Beringian bison. We therefore extended the Bayesian coalescent method (*26*) to a two-epoch demographic model with exponential population growth at rate r_{early}, until a transition time, t_{trans}, after which a new exponential rate, r_{late}, applies until the present effective population size, N_0, is reached (Fig. 2A). In this model, both the early and late epochs can have positive or negative growth rates, with both the rates and the time of transition estimated directly from the data.

The analysis strongly supported a boom-bust demographic model (Table 1), in which

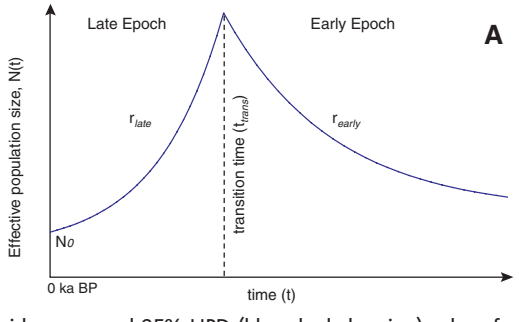

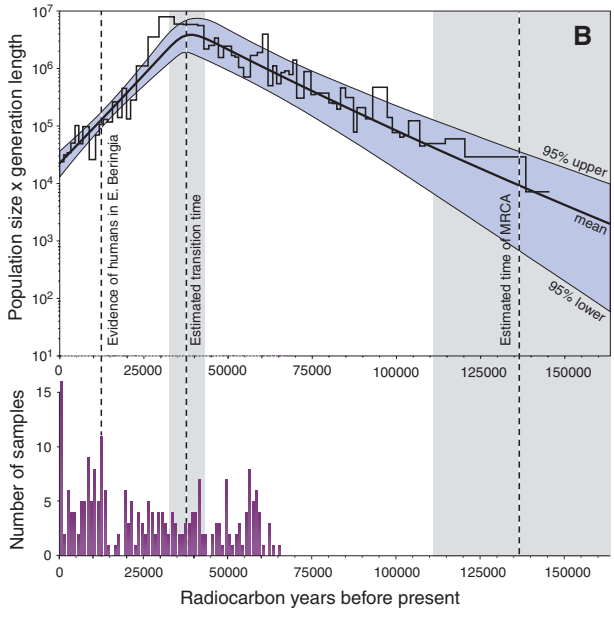

Fig. 2. (**A**) The two-epoch demographic model with four demographic parameters: N_0, r_{early}, r_{late}, and t_{trans}. The effective population size is a compound variable considered linearly proportional to census population size. (**B**) Log-linear plot describing the results of the full Bayesian analyses. Smoothed curves provide mean and 95% HPD (blue-shaded region) values for effective population size through time. Dashed vertical lines and gray-shaded regions describe mean and 95% HPD for the estimated time of the MRCA (111 to 164 ky B.P.), transition time (32 to 43 ky B.P.), and the earliest unequivocal reported human presence in eastern Beringia (~12 ky B.P.) (*5*). The stepped line is the generalized skyline plot derived from the maximum a posteriori tree of the exponential growth analysis. The bar graph shows the number of radiocarbon-dated samples in bins of 1000 radiocarbon years. No relation is apparent between the absolute number of samples and the estimated effective population size or transition time.

Table 1. Results of Bayesian analyses assuming constant population size, exponential growth, and a two-epoch model for the full analysis of 191 bison associated with finite radiocarbon dates (*14*). Model parameters are as defined in (*26*). The large difference between the mean goodness-of-fit statistics [ln(posterior)] indicates that under either the Akaike information criterion or Bayesian information criterion tests, the two-epoch model is a significantly better fit to the data than the simpler models.

	Constant size			Exponential growth			Two epoch		
	Lower	Mean	Upper	Lower	Mean	Upper	Lower	Mean	Upper
Age estimates (yr B.P.)									
Root height	117,000	152,000	189,000	113,000	146,000	181,000	111,000	136,000	164,000
Modern/southern clade	20,200	28,000	36,600	18,600	26,400	35,000	15,400	23,200	32,200
Eurasian clade	85,000	116,000	151,000	83,000	112,000	144,000	89,000	114,000	141,000
Model parameters									
Mean ln(posterior)		−6530.795			−6517.35			−6394.568	
Mutation rate (substitutions/site/year)	2.79×10^{-7}	3.78×10^{-7}	4.85×10^{-7}	2.30×10^{-7}	3.20×10^{-7}	4.13×10^{-7}	2.30×10^{-7}	3.20×10^{-7}	4.13×10^{-7}
Kappa	19	27	37	19	27.4	37	19	27	37
Shape parameter	0.22	0.35	0.49	0.22	0.35	0.49	0.22	0.35	0.5
Proportion of invariant sites	0.33	0.45	0.56	0.33	0.45	0.56	0.34	0.45	0.56

an exponential expansion of the bison population was followed by a rapid decline, with a transition around 37 ky B.P. (Fig. 2B). At the height of the boom, the population size was around 230 times (95% HPD: 71 to 454 times) that of the modern population. When this model is applied to the modern clade alone, a growth period peaks around 1000 years ago (95% HPD: 63 to 2300 yr B.P.) and is followed by a rapid decline (*14*), which is consistent with historical records of a population bottleneck in the late 1800s (*13*). These results illustrate the power of this method to recover past demographic signals.

The effects of population subdivision and patch extinction and recolonization on coalescence patterns have not been fully characterized, yet they can influence demographic estimates such as skyline plots (*27*). To test for the effect of population subdivision on our models, the two-epoch analysis was repeated first without the Eurasian bison and then without both Eurasian and central North American bison. The results of these analyses were consistent with those for the entire data set (*14*), suggesting that the assumption of panmixia does not affect the analysis. These results suggest that the major signal for the boom-bust scenario came from the well-represented eastern Beringian population.

The timing of the decline in Beringian bison populations (Fig. 2B) predates the climatic events of the LGM and events at the Pleistocene-Holocene boundary. The bison population was growing rapidly throughout MIS 4 and 3 (~75 to 25 ky B.P.), approximately doubling every 10,200 (95% HPD: 7500 to 15,500) years. The reversal of this doubling trend at 42 to 32 ky B.P. and the subsequent dramatic decrease in population size are coincident with the warmest part of MIS 3, which is marked by a reduction in steppe-tundra due to treecover reaching its late Pleistocene maximum (*28*). Modern boreal forests serve as a barrier to bison dispersal because they are difficult to traverse and provide few food sources (*3*). After the interstadial, cold and arid conditions increasingly dominated, and some component of these ecological changes may have been sufficient to stress bison populations across Beringia. Previous reports of local extinction of brown bears (*29*) and hemionid horses (*8*) in Alaska around 32 to 35 ky B.P. support the possibility of a larger scale environmental change affecting populations of large mammals.

These results have considerable implications for understanding the end-Pleistocene mass extinctions, because they offer the first evidence of the initial decline of a population, rather than simply the resulting extinction event. These events predate archaeological evidence of significant human presence in eastern Beringia (*5*), arguing that environmental changes leading up to the LGM were the major cause of the observed changes in genetic diversity. If other species were similarly affected, differences in how these species responded to environmental stress may help to explain the staggered nature of the megafaunal extinctions (*7*, *30*). However, it is possible that human populations were present in eastern Beringia by 30 ky B.P., with reports of human-modified artifacts as old as 42 to 25 ky B.P. from the Old Crow basin in Canada's Yukon Territory (*31*). Although the archaeological significance of these specimens is disputed and the number of individuals would be low, the specimens are consistent with the timing of the population crash in bison. This emphasizes that future studies of the end–Pleistocene mass extinctions in North America should include events before the LGM.

Ancient DNA is a powerful tool for studying evolutionary processes such as the response of organisms to environmental change. It should be possible to construct a detailed paleoecological history for late Pleistocene Beringia using similar methods for other taxa. Almost none of the genetic diversity present in Pleistocene bison survived into Holocene populations, erasing signals of the complex population dynamics that took place as recently as 10,000 years ago.

References and Notes

1. G. Hewitt, *Nature* **405**, 907 (2000).
2. R. W. Graham *et al.*, *Science* **272**, 1601 (1996).
3. R. D. Guthrie, *Frozen Fauna of the Mammoth Steppe* (Univ. of Chicago Press, Chicago, 1990).
4. G. D. Zazula *et al.*, *Nature* **423**, 603 (2003).
5. D. R. Yesner, *Quat. Sci. Rev.* **20**, 315 (2001).
6. B. W. Brook, D. Bowman, *J. Biogeogr.* **31**, 517 (2004).
7. J. Alroy, *Science* **292**, 1893 (2001).
8. R. D. Guthrie, *Nature* **426**, 169 (2003).
9. J. N. McDonald, *North American Bison: Their Classification and Evolution* (Univ. of California Press, Berkeley, CA, 1981).
10. C. A. S. Mandryk, H. Josenhans, D. W. Fedje, R. W. Matthewes, *Quat. Sci. Rev.* **20**, 301 (2001).
11. A. S. Dyke *et al.*, *Quat. Sci. Rev.* **21**, 9 (2002).
12. M. F. Skinner, O. C. Kaisen, *Bull. Am. Mus. Nat. Hist.* **89**, 126 (1947).
13. F. G. Roe, *The North American Buffalo,* (Univ. of Toronto Press, Toronto, ON, ed. 2, 1970).
14. Materials and methods are available as supporting material on *Science* Online.
15. D. M. Lambert *et al.*, *Science* **295**, 2270 (2002).
16. D. G. Bradley, D. E. MacHugh, P. Cunningham, R. T. Loftus, *Proc. Natl. Acad. Sci. U.S.A.* **93**, 5131 (1996).
17. C. S. Troy *et al.*, *Nature* **410**, 1088 (2001).
18. J. A. Burns, *Quat. Int.* **32**, 107 (1996).
19. M. C. Wilson, *Quat. Int.* **32**, 97 (1996).
20. J. C. Driver, in *People and Wildlife in Northern North America*, S. C. Gerlach, M. S. Murray, Eds. (British Archaeological Reports, International Series 944, Archaeopress, Oxford, 2001), pp. 13–22.
21. N. Catto, D. G. E. Liverman, P. T. Bobrowsky, N. Rutter, *Quat. Int.* **32**, 21 (1996).
22. L. A. Halsey, D. H. Vitt, I. E. Bauer, *Clim. Change* **40**, 315 (1998).
23. R. O. Stephenson *et al.*, in *People and Wildlife in Northern North America*, S. C. Gerlach, M. S. Murray, Eds. (British Archaeological Reports, International Series 944, Archaeopress, Oxford, 2001), pp. 125–148.
24. R. C. Griffiths, S. Tavare, *Philos. Trans. R. Soc. London Ser. B* **344**, 403 (1994).

25. K. Strimmer, O. G. Pybus, *Mol. Biol. Evol.* **18**, 2298 (2001).
26. A. J. Drummond, G. K. Nicholls, A. G. Rodrigo, W. Solomon, *Genetics* **161**, 1307 (2002).
27. J. R. Pannell, *Evolution* **57**, 949 (2003).
28. P. M. Anderson, A. V. Lozhkin, *Quat. Sci. Rev.* **20**, 93 (2001).
29. I. Barnes, P. E. Matheus, B. Shapiro, D. Jensen, A. Cooper, *Science* **295**, 2267 (2002).
30. D. K. Grayson, D. J. Meltzer, *J. Archaeol. Sci.* **30**, 585 (2003).
31. R. E. Morlan, *Quat. Res.* **60**, 123 (2003).
32. We thank the museums and collections that donated material and T. Higham, A. Beaudoin, K. Shepherd, R. D. Guthrie, B. Potter, C. Adkins, D. Gilichinsky, R. Gangloff, S. C. Gerlach, C. Li, N. K. Vereshchagin, T. Kuznetsova, G. Boeskorov, the Alaska Bureau of Land Management, and the Yukon Heritage Branch for samples, logistical support, and assistance with analyses. We thank D. Rubenstein, R. Fortey, and P. Harvey for comments on the manuscript; Balliol College; the Royal Society; the Natural Environment Research Council; the Biotechnology and Biological Sciences Research Council; Rhodes Trust; Wellcome and Leverhulme Trusts for financial support; and Oxford Radiocarbon Dating Service and Lawrence Livermore National Laboratory for carbon dating.

Supporting Online Material
www.sciencemag.org/cgi/content/full/306/5701/1561/DC1
Materials and Methods
SOM Text
Figs. S1 to S5
Tables S1 to S4
References

4 June 2004; accepted 4 October 2004

Periodical Cicadas as Resource Pulses in North American Forests

Louie H. Yang

Resource pulses are occasional events of ephemeral resource superabundance that occur in many ecosystems. Aboveground consumers in diverse communities often respond strongly to resource pulses, but few studies have investigated the belowground consequences of resource pulses in natural ecosystems. This study shows that resource pulses of 17-year periodical cicadas (*Magicicada* spp.) directly increase microbial biomass and nitrogen availability in forest soils, with indirect effects on growth and reproduction in forest plants. These findings suggest that pulses of periodical cicadas create "bottom-up cascades," resulting in strong and reciprocal links between the aboveground and belowground components of a North American forest ecosystem.

Ecologists are increasingly investigating the effects of resource pulses in natural systems (*1*). Examples of resource pulses include mast years of unusually heavy seed production (*2*–*4*), eruptive plant growth after El Niño rainfalls (*5*–*8*), postspawning salmon mortality in riparian communities (*9*, *10*), and large-scale insect outbreaks (*3*, *11*–*13*). Despite great variation in the specific characteristics of these resource pulses, each represents a brief, infrequent event of high resource availability. Resource pulses are of broad interest because they provide extreme examples of the spatiotemporal variability inherent in all ecosystems. Recent theoretical efforts have suggested that many communities may be strongly influenced by transient dynamics after ecological perturbations (*14*, *15*), and empirical studies in diverse systems have demonstrated that resource pulses are often substantial perturbations with strong effects on consumer populations, especially among opportunistic generalist species (*1*).

Resource pulses have well-documented effects on aboveground consumers, and they may also provide important inputs to belowground systems (*1*, *16*). In many pulsed systems, only a small proportion of resource biomass is consumed aboveground (*17*–*19*), and aboveground predator satiation during resource pulses could allow large belowground inputs. Many belowground organisms are well-adapted to take advantage of resource pulses because of their high intrinsic rates of growth and rapid foraging responses (*20*, *21*). Studies in natural systems support the idea that aboveground resource pulses may contribute to belowground systems. For example, mast events in boreal forests produce large inputs of rapidly decomposed spruce seeds that increase soil nitrogen availability (*22*), and large-scale gypsy moth outbreaks in temperate forests influence nutrient cycling through defoliation and frass deposition (*11*).

The role of arthropods in regulating plant inputs and facilitating decomposition is widely acknowledged (*21*), although most ecologists have assumed that arthropod bodies are an unimportant ecosystem biomass component (*23*). However, the unusual life history of periodical cicadas suggests that they may be a substantial, temporally stored resource pulse. Periodical cicadas are the most abundant herbivores in North American deciduous forests in both number and biomass (*24*), but their role in forest ecosystems is largely unrecognized because of their long belowground life history. Adult periodical cicadas emerge synchronously across large geographic areas, or "broods," often on a scale of 10^5 km^2. The spatial distribution of cicadas is highly variable and dynamic on small scales (<1 km) and is influenced by fragmentation in forest habitats (*17*, *23*–*26*). Yet, cicadas are broadly distributed across a large and diverse area, with a cumulative range encompassing much of the eastern United States (fig. S1). Adult cicadas are aboveground for less than 6 weeks (*26*). Cicada emergence densities ranging from 3 to 350 cicadas m^{-2} are well documented (*26*), and most cicadas escape predation at high densities (*17*, *18*). Direct measures of cicada densities in 2002 and 2004 support previously reported density estimates (*27*). In dense populations, the cumulative biomass of periodical cicadas is among the greatest of any terrestrial animal (*24*) and represents a substantial flux of high-quality biomass (*23*, *28*, *29*). Little is known about the belowground effects of this resource pulse.

Here, I investigate the direct belowground and indirect aboveground effects of cicada litter inputs resulting from cicada resource pulses. I conducted field experiments during three con-

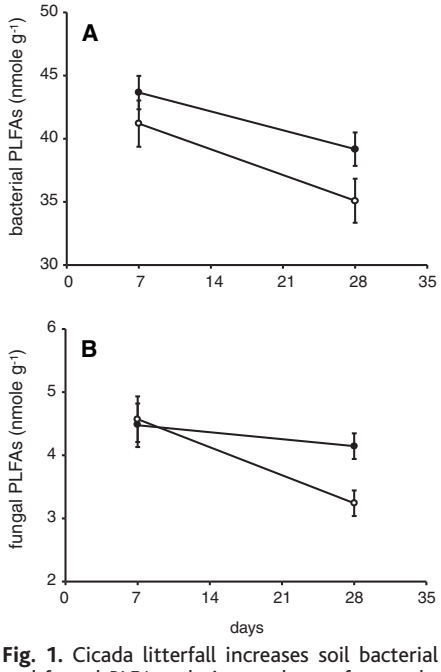

Fig. 1. Cicada litterfall increases soil bacterial and fungal PLFAs relative to those of controls, indicating increased microbial biomass. (**A**) Bacterial PLFAs in cicada-supplemented and control plots 7 and 28 days after experimental cicada pulse. (**B**) Fungal PLFAs in cicada-supplemented and control plots 7 and 28 days after experimental cicada pulse. Open circles represent control plots, and filled circles represent plots receiving 120 cicadas m^{-2}. Error bars show mean ± SE.

Center for Population Biology, Section of Evolution and Ecology, University of California, One Shields Avenue, Davis, CA 95616, USA. E-mail: lhyang@ucdavis.edu